Chapter 9
Channel Stability Assessment and Stabilization Measure of Mersa River, Ethiopia

Getanew Sewnetu

Abstract The objective of this study is to evaluate channel stability and recommend appropriate mitigation measures for the Mersa River, in Awash River Basin, Ethiopia. The HEC-RAS5.0.7 model was used to evaluate the Mersa riverbed and bank stability, quantify the depth or mass sediment erosion amount, and identify flood-prone areas. To achieve this objective, both field investigations, such as river cross-section data collection and soil sample collection, and experimental tasks, such as sieve analysis and triaxial compression tests, were carried out. The HEC-RAS model simulation with the Yang sediment transport formula is the best fit for the study compared to the Meyer, Peter, and Muller sediment transport methods. For the entire simulation period, the average aggradation was 1.24 m and 0.98 m in the upstream and downstream reaches, respectively, whereas the average degradation in both the upstream and downstream reaches was 1.25 m. The average sediment erosion generated by the Mersa River was 22.47 kt/yr. Both aggradation and degradation were observed in the study reach, but the Mersa River reach was more affected by erosion than deposition. Mersa riverbank stability and toe erosion assessed by BSTEM of HEC-RAS were safe, and the bank toe neither aggraded nor degraded in response to the flow. Additionally, the water surface of the Mersa River was computed using steady flow analysis, showing that floods over the top above the bank and adjacent area (Mersa town) were affected by floods, and the reality was also true. It was shown that there was farmland loss and property damage due to floods. Finally, this investigation showed that the channel bed was unstable while the bank was stable. Different stabilization measures, such as the Gabion bank, check dam, and drop structure, were recommended to prevent flood-prone areas from experiencing floods and to control channel bed instability.

Keywords Sieve analysis · Triaxial compression test · Channel bed and bank stability · HEC-RAS model · BSTEM · Aggradation and degradation · Stabilization measure

G. Sewnetu (✉)
Department of Hydraulic and Water Resources Engineering, Woldia University, Woldia, Ethiopia
e-mail: getanew.s@wldu.edu.et

A. M. Melesse et al. (eds.), *Land and Water Degradation in Ethiopia*, Springer Geography, https://doi.org/10.1007/978-3-031-60251-1_9

Study Area Description

Location

The Mersa River is found in the western highlands of the Awash Terminal, the subbasins of the A wash basin (Fig. 9.1). The Mersa River originates from mountains and drains to the downstream passes in Mersa town. Mersa town is found in North Wollo, Amhara region, Ethiopia, 495 km from Addis Ababa and is geographically located at 11° 40′ N latitude and 39° 39.5′ E longitude and 1600 m elevation mean above sea level. Mersa is situated along country (Ethiopian) Highway 2, and the highway passes in the Mersa River.

The watershed is delineated using HEC-GeoHMS, which is an extension of ArcGIS (for this thesis, ArcGIS 10.4 was used) with a 30 m resolution digital elevation model (DEM).

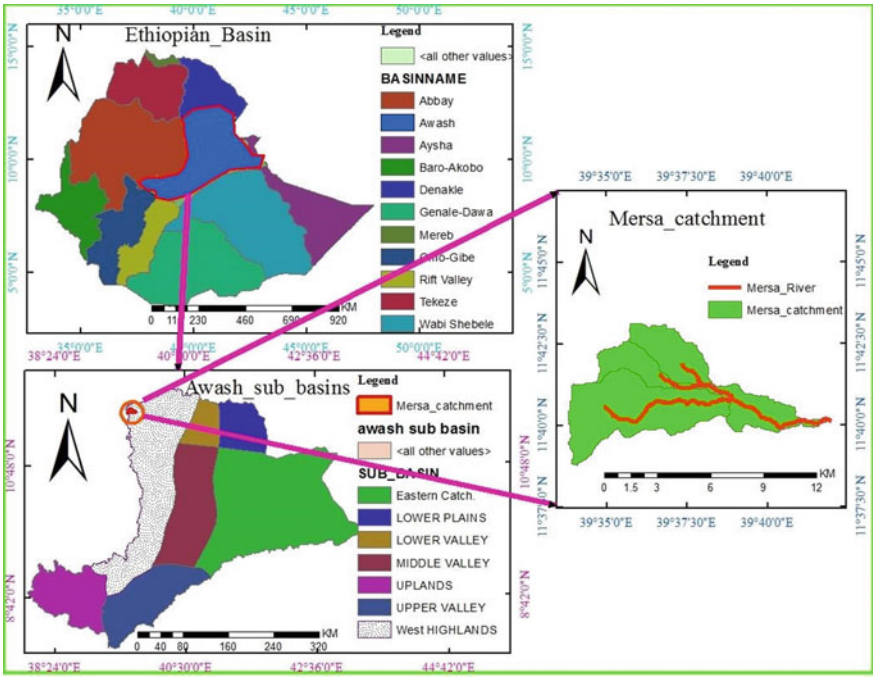

Fig. 9.1 Location of the Mersa catchment

Soil

The earth material (soil) in the Mersa catchment is grounded on soil type criteria eutric cambisols, eutric regosols, leptosols, and vetric cambisols, while according to texture, sandy loam and gravel have the greatest coverage in the watershed of Mersa. Figure 9.2 shows a soil map of the watershed.

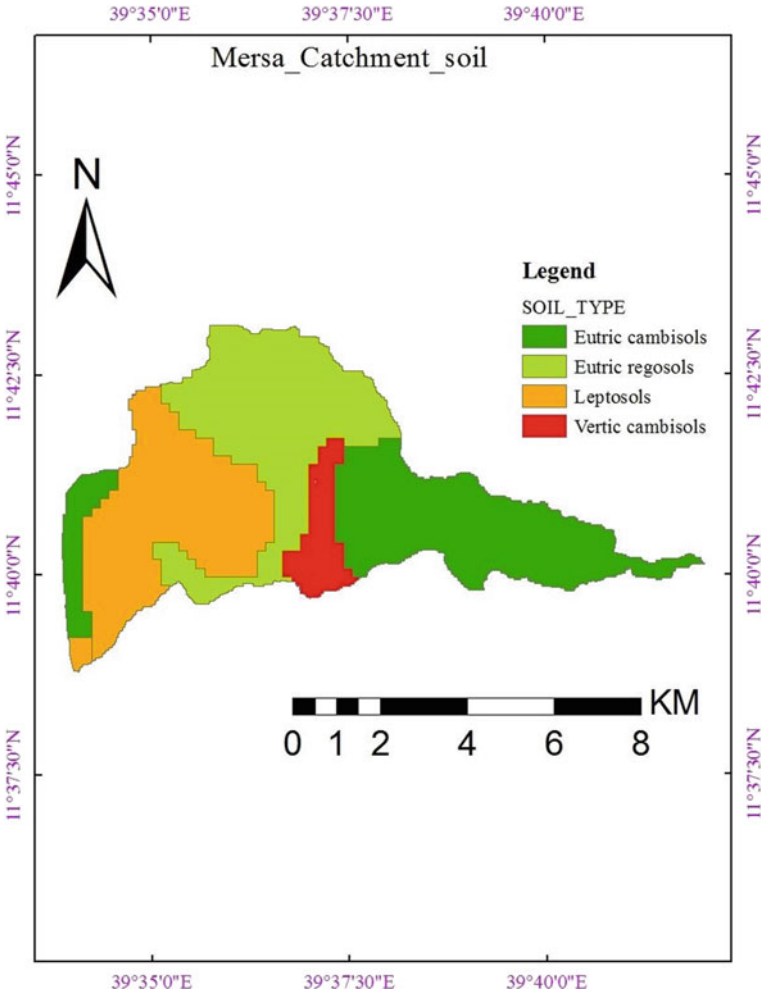

Fig. 9.2 Soil map of the Mersa catchment

Table 9.1 Geological formation of the Mersa catchment

No.	Symbol	Stratigraphy	Age	Lithology	Description
1	P2a	Cenozoic volcano	Eocene	ASHANGI Formation	Deeply weathered alkaline and transitional basalt flows with rare intercalations of tuff, often tilted (includes Akobo Basalts of SW Ethiopia)
2	P3a	Cenozoic volcano	MIDDLE–LATE OLIGOCENE	AIBA Basalts	Flood basalts with rare basic tuff
3	PNa	Cenozoic volcano	OLIGOCENE–MIOCENE	ALAGE formation	Transitional and subalkaline basalts with less rhyolite with trachyte eruptive

Geology

The geological situation is the basis and cornerstone of river stability investigations. Any stratigraphic classification of water-bearing formations should begin from lithological classifications by accounting for geological arrangements such as faults, joints, folds, and other tectonic features with hydrological importance.[1]

According to age, the geological formation in the study watershed includes EOCENE, MIDDLE–LATE OLIGOCENE, and OLIGOCENE–MIOCENE[2,3]. The general description of the geological state of the study catchment is compiled in Table 9.1.

Land Use and Land Cover

The land usage and coverage of the Mersa catchment (Fig. 9.3) was prepared under ArcGIS 10.4. First, a Landsat 8 image from the USGS earth explorer (http://earthexplorer.usgs) was created to account for any area desired for the latest or updated image

[1] Ethiopia Health Infrastructure Program, Health Centres Groundwater Investigation Final Report February 2016.

[2] www.ethiogrio.com/files//Ethiopia_Map_251592290.pdf

[3] Identification and Engineering Geological Studies of Small Hydropower Sites in Muger, Jemma and Waleka Sub-Basins (Central Ethiopia) By Nehemia Solomon.

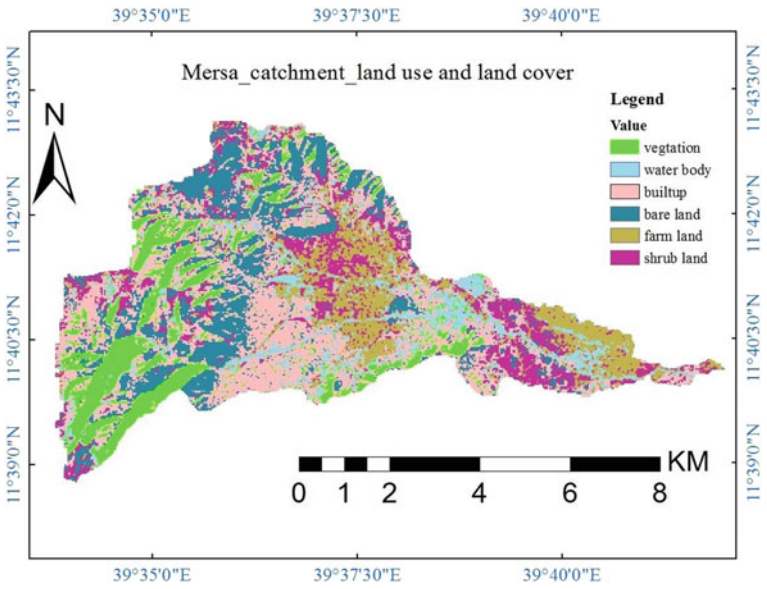

Fig. 9.3 Land use and land cover of the Mersa catchment

for this investigation. The image released on February 27, 2019, was downloaded and used to composite the 11 downloaded bands, and the image classification method was unsupervised classification. Finally, by relating the composite to the real image at Google Earth, the land use and land cover were prepared.

Climate

The minimum and maximum temperatures in the catchment are 10 °C and 34 °C, respectively. The district receives average yearly rainfall ranging from 350–835 mm. The main rainy season is from June to the end of September. The mean annual wind speed, relative humidity and solar radiation in the catchment are 2.5 m/sec, 0.506, and 26 MJ/m^2, respectively.

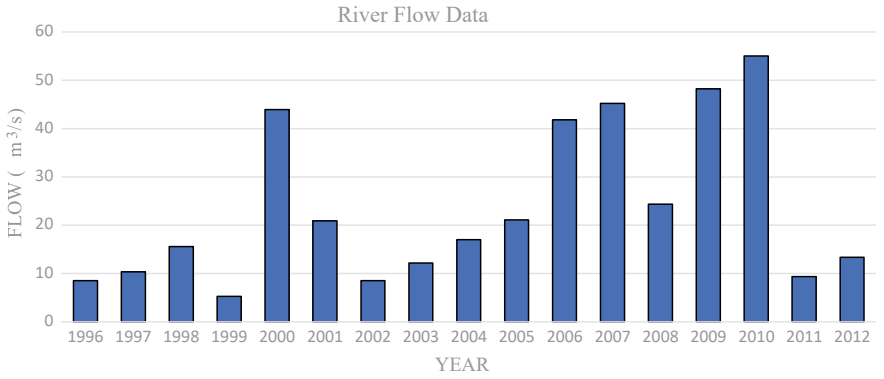

Fig. 9.4 Annual maximum mean daily river flow data of the Mersa River

Data Collection

Hydrology

The recorded flow data were collected from the Minster of Water, Irrigation, and Electricity for the Mersa River between 1996 and 2012, and the annual maximum mean daily instantaneous flow data (Fig. 9.4) were used to estimate the dominant and bank full discharge of the river.

Soil Sample for Gradation and Triaxial Compression Test

The possible representative soil sample is taken from the riverbed, left side, and right side bank for gradation analysis at six different places to obtain the possible accurate data regarding the soil characteristics of the selected 2.6 km channel reach so at left, right, and riverbed for each taken at two different places, while the triaxial compression experiment sample is taken from the riverbank at three different places.

Geometric Data

River Cross-Section Data

Channel cross-section data are essential inputs in the HEC-RAS model, so for this study, 42 reach sections were taken along a 2.6 km interval from 50 to 100 m depending on river meandering and straightness conditions.

The cross-section data contain the station number, y distance of the point from a reference point and z elevation. The downstream reach length is calculated from the difference between two successive coordinates y or the distance of the points.

Generally, the river of Mersa in the first two reaches is narrow, while beginning from the 3rd station to station 26, it becomes very wide, and between stations 26 and 27, there is a Multi Span RC Deck Girder Bridge structure with a span length of 42.8 m, bridge opening length of 22.5 m and bridge width of 8 m.

Manning Roughness Coefficient

The Manning roughness coefficient is another basic input for the HEC-RAS model setup, but the challenge is earning the exact value for the stream because the roughness coefficient depends on the channel grade of irregularity, variations in the channel cross-section, relative to effective obstructions, vegetation, and meandering degree. According to Chow (1959), the surface roughness coefficient value can be calculated by considering the existing channel physical characteristics, such as surface roughness, vegetation, obstruction, channel alignment and channel bank, and bed materials. Considering various primary variables affecting the roughness coefficient, Manning's n value can be calculated using

$$n = (n_0 + n_1 + n_2 + n_3 + n_4)m_5 \tag{9.1}$$

where n_0 = is a basic n value for a straight, uniform, smooth channel in the natural materials involved (Chow 1959) and n_1 = is a value added to n_o to correct for the effect of surface irregularities (Chow 1959).

n_2 is a value for variations in the shape and size of the channel cross-section, (Chow 1959) n_3 is a value for obstructions, (Chow 1959) n_4 is a value for vegetation and flow conditions, (Chow 1959) and m_5 is a correction factor for meandering of the channel (Chow 1959).

The basic n_0 is calculated in the empirical formula developed from the channel bank and bed soil material that is done at sieve analysis, whereas starting from n_1 to m_5 estimated from Table 9.2.

According to French (1986), the basic n_0 is calculated by the following empirical equation. $n_0 = 0.038 * {d_{90}}^{1/6}$ d in metermetres Meyer Peter and Muller (1948) $n_0 = 0.039 * {d_{50}}^{1/6}$ d in feet Garde and Ranga Raju (1978) $n_0 = 0.047 * {d_{50}}^{1/6}$ d in meters,

where d_i is the grain soil size, in which i is the percentage of material by weight finer than d.

For illustration, Manning's roughness n of the Mersa River upstream of the channel bed at station 42.

The other values are carefully chosen from Table 9.3: $n_1 = 0.005$, moderate degree of irregularity $n_2 = 0.013$, channel cross-section varies occasionally $n_3 = 0.02$, obstruction is negligible except at the bridges, which will be considered separately $n_4 = 0.007$, vegetation effect $m = 1.00$, and degree of meandering is minor.

Table 9.2 Gradation result at cross-section 42

Sieve size	Soil laboratory gradation result
D90 (mm)	8.4015
D90 (m)	0.00840
D50 (mm)	3.1664
D50 (ft)	0.0104
D50 (m)	0.0032
Garde and Raju	0.0182
Subramanya	0.0180
Meyer Peter and Muller	0.0171
Average n_0	0.018

Table 9.3 Contraction and expansion for various channel conditions

Channel condition	Coefficient	
	Expansion	Contraction
Gradual change	0.3	0–0.1
Abrupt change	0.5	0.5

Then, $n = (0.018 + 0.005 + 0.013 + 0.02 + 0.007) \times 1.00 = 0.065$. For the remaining channel reach, Manning's roughness values were estimated in a similar fashion as above.

Coefficients of Contraction and Expansion

According to Chow (1959), the recommended contraction and expansion coefficients for different channel conditions are presented in Table 9.3 (Fig. 9.5).

Data Analysis

Analysis of data is essential for the future to process in model application, and it simply examines the data quality, sufficiency, quantity, etc. According to Hawi (2018), data analysis assesses data by means of analytical logical reasoning to examine each component of the data provided. Data analysis is the first and essential of several steps that must be carried out when conducting a research experiment. Data from several sources are collected, reviewed, and analyzed to form some findings or conclusions. For the 17-year sample stream flow data of the Mersa River analyzed in this study, there were no high outliers or low outliers.

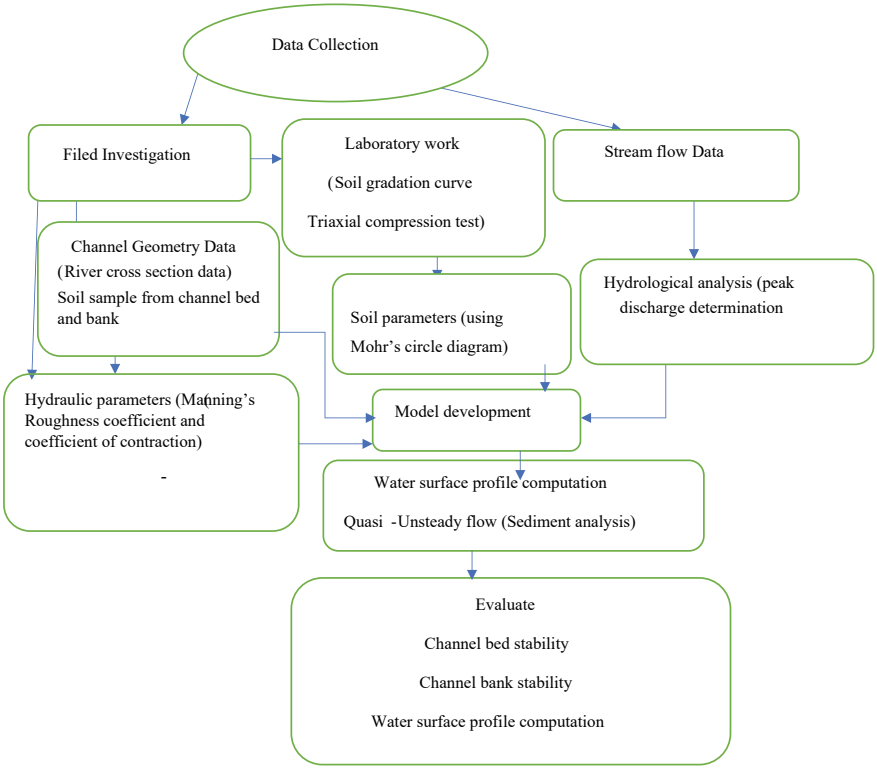

Fig. 9.5 Conceptual framework

Hydrologic Analysis

The maximum design flood is the river peak discharge that corresponds to a certain recurrence interval, which is important in the practical design of all irrigation and hydraulic structures (Subramanya 2008).

Frequency Analysis of Floods

It is one method to estimate the extreme flood of the channel that is utilized to design any hydraulic structure (Brunner 2016). Flow in the watershed is dependent on the characteristics of the watershed, rainfall and antecedent humidity condition individually, and these factors in turn bank on a list of constituent variables. This makes the estimation of the flood peak a very complex problem, leading to different approaches. The empirical formula and unit hydrograph method have been described in the previous chapter. Another approach to the prediction of flood flow is frequency analysis, which must consider all catchment factors. In frequency analysis approaches, the common problem is to forecast extreme flood events. Toward the extreme, specific extreme value distributions are supposed, the desired statistical

parameters are estimated from available data, and the flood magnitude for the specific return period is estimated. The 17 successive year stream gauged data are analyzed for the outlier test next, and the peak flood for different return periods would be computed as follows, but before this, to which method of frequency flood analysis the recorded is fitted must be carried out primarily using the l-moment ratio diagram.

L-Moment Ratio Diagram

It is a diagram based on the coefficient of skewness (Cs) versus the coefficient of kurtosis to identify appropriate distributions. L-moment ratio diagram plotted for a given regional sample size. The identification of a parent dispersion can be achieved much more easily by using an L-moment ratio diagram, especially for skewed distributions. Some useful relationships for constructing diagrams of the L-moment ratio for some common distributions are given by Hosking (1990, 1991).

From the L-moment ratio diagram analysis shown below, the collected stream gauged data best fit the general extreme value (Gumbel's method) (Fig. 9.6).

Soil Laboratory Analysis

Generally, the laboratory analysis category in to two for this research, i.e., the soil gradation (particle size distribution) and triaxial compression test. Both gradation curve and triaxial compression tests were carried out at Woldia University, Civil Engineering Department, Soil Laboratory.

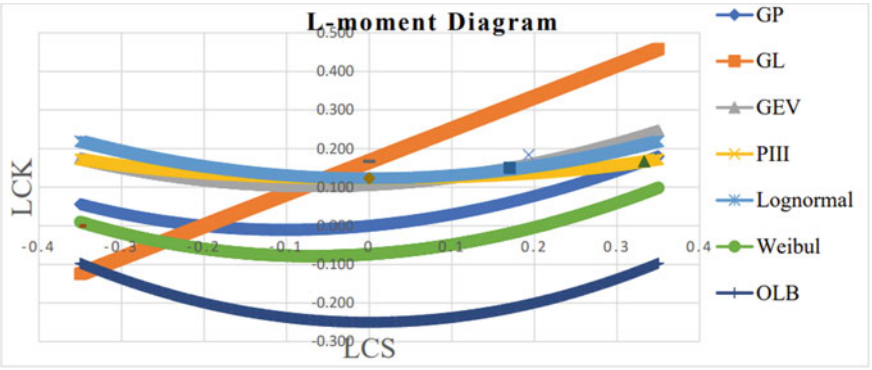

Fig. 9.6 L-moment ratio diagram

Soil Gradation Analysis

A soil gradation curve is performed to estimate the percentage of different grain sizes contained within the soil. As discussed above for the bed river, the left bank and right channel bank of the Mersa River sample were taken at 2 different places for each, and finally, a total sample was taken at six places.

For this research, the cone dimeter used started from pan, 0.075–9.5 mm according to Arora (2008) coarse-grained soils (size > 4.75 mm) and sand fraction (75 μm < size < 4.75 mm), so the soil retained above sieve diameter 4.75 mm was considered gravel, the soil retained in between sieve diameter 0.106–4.75 mm was considered sand, and the soil retained at sieve diameter 0.075 mm and at the pan was considered fine soil.

The laboratory results of sieve analysis were grouped into two broad classes: riverbank and riverbed material. Gradation curve of soil for six representative soil samples taken from different places to determine the proportion of gravel, sand, and fine parts of the soil material. The study channel reach has two parts: the upper reach and lower reach, so samples were taken from the upper three parts of the left riverbank, right riverbank and riverbed soil, and samples were also taken in the same way from the lower channel reach.

1. Riverbed material composition

The gradation curve analysis result of the bed material composition characterized by coarse grains, including sand and gravel, shows that the bed material above 95% of the total sample was coarser with particle grain sizes greater than 0.075 mm.

As shown in Table 9.4 and Fig. 9.7, for the soil particles in the upper reach of the Mersa riverbed soil material, the percentages of gravel, sand and fine soil material are 43.23 with particle sizes larger than 4.75 mm, 54.39 with particle grain sizes in the range between 0.075 mm and 4.75 mm, and 2.38 with particle sizes less than 0.075 mm, respectively, showing that more than 95% of the bed material is gravel and sand. D84, D50, and D16 indicate particle sizes of 7.74, 3.16, and 0.32, respectively, at which 84%, 50%, and 16% of the soil materials are finer than this size. In the same method, the gradation curve result for the bed sediment composition of the lower channel reach showed that the coarse-grained soil was dominated by sand (fine sand to very coarse sand) and gravel (from very fine gravel to medium gravel). The uniformity coefficients (D60/D10) for both the upstream and lower reaches were 23 and 14, respectively, for sand and gravel, which had uniformity coefficients greater than 6 for sand and 4 for gravel, showing well-graded coarse-grained soil.

Triaxial Compression Test Analysis

The triaxial compression test is used to determine the shear parameters in soils under various drainage conditions. A triaxial compression test is necessary to determine the soil parameters that affect the soil shear strength. Shear strength is the primary engineering property that controls soil mass stability under loading (Arora 2008). According to (Murthy 2002), the shear strength parameter c is cohesion, and ϕ is the angle of shearing resistance of soils either in the undisturbed or remolded states.

Table 9.4 Upper reach riverbed material particle size curve analysis

Sieve No.	Sieve diameter	Mass of empty sieve (g)	Mass of sieve + soil retained (g)	Soil retained (g)	Mass cumulative retained (g)	Percent retained (%)
	9.5	495.8	495.8	0	0	0
4	4.75	460.5	698.5	238	238	43.24
10	2	402.6	467.2	64.6	302.6	54.99
20	0.84	386.5	445.3	58.8	361.4	65.66
40	0.425	391.6	455.6	64	425.4	77.29
60	0.25	384.1	447.7	63.6	489	88.84
140	0.106	363.5	398.2	34.7	523.7	95.15
200	0.075	357.5	371.1	13.6	537.3	97.62
pan		352.6	365.7	13.1	550.4	100
Total		3242.1	3779.4	537.3	2877.4	522.79

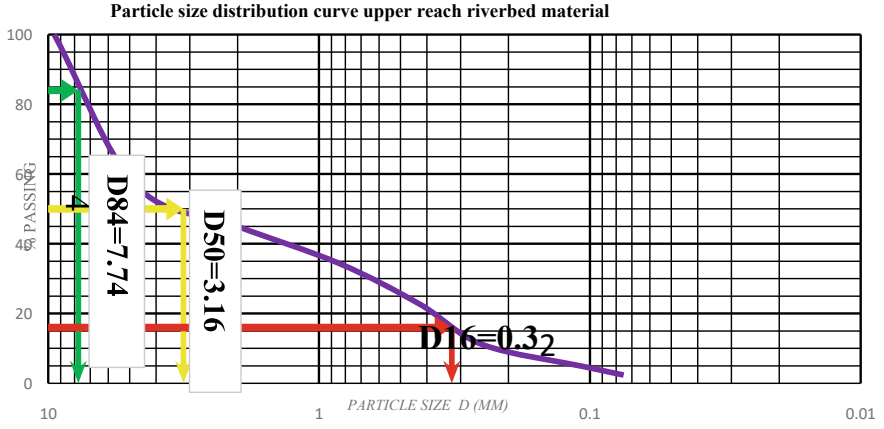

Fig. 9.7 Grain size distribution curve of the upper reach riverbed material

For this research, disturbed soil was taken from the Mersa reach and remolded in the laboratory. The soil sample was taken at 3 different places from the riverbank for the triaxial compression test.

Soil parameter cohesion c and angle of internal friction ϕ are essential inputs for the BSTEM model that should be determined in the laboratory. As defined earlier, the triaxial compression test is used to determine the soil parameter or variables (c and ϕ). Specifically, for this study, triaxial compression tests were performed on riverbank soil samples under 50, 100, and 200 kN load conditions. Although the experiment (triaxial compression test) was not adequate to determine the soil strength parameter, it requires Mohr's circle analysis with these experimental results. According to Arora (2008), Mohr's circle is a diagram or graphical technique for the estimation of stresses

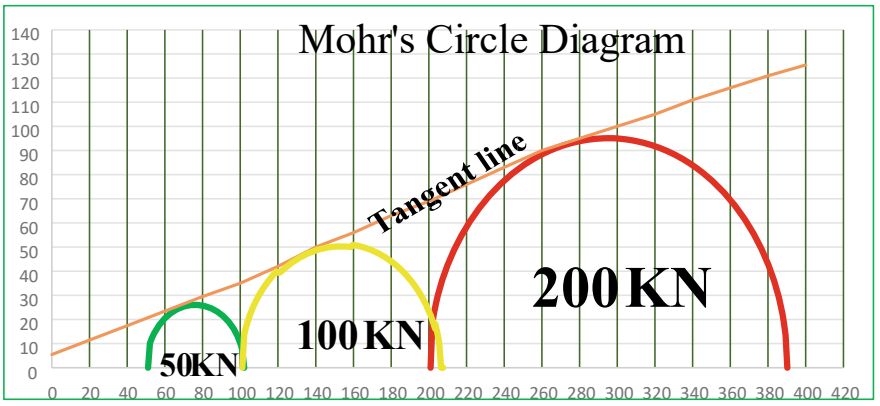

Fig. 9.8 Mohr's circle diagram for different axial loads (50, 100 and 200 kN)

on a plane inclined to the principal planes. By drawing the Mohr's circle, the three-test result in a single graph as presented below soil shear strength variables or parameter become cohesion, $C = 5.46$ kPa and shearing resistance angle, $\phi = 14°$ (Fig. 9.8)

HEC-RAS Model Development

As discussed in the previous chapter, HEC-RAS allows users to perform one-dimensional steady flow to water flow surface profile computations, unsteady flow simulations, quasiunsteady sediment transport/mobile boundary computations, and water quality analyses (Brunner 2016). For this study, a 1D HEC-RAS model is developed to compute sediment transport capacity, to predict riverbed changes by using sediment balance equations and to assess the water surface profile.

Steady Flow Analysis and Flood Inundation Map

Steady Flow Simulation

The energy equation is used to compute the water flow surface profile. This is solved by an iterative procedure, which is called the direct standard step method from one cross-section to the other (Brunner 2016). The model also uses the Manning equation to compute water discharge (Brunner 2016).

The surveyed cross-section collected data were used to establish a 1D steady flow model for different discharge scenarios to analyze the water level in all reaches. The discharge computed by GEV is used for the upstream boundary and the downstream boundary condition of the normal depth, which is determined from the longitudinal

Table 9.5 Steady flow upstream boundary conditions

Return period (year)	Discharge (m^3/s)
Upstream boundary condition	
2	41
10	68
50	91
100	101

slope of the river reach. The discharge used in the steady flow analysis is shown in Table 9.5 with a return period of 2–100 years.

The water surface profile for 2-, 10-, 50-, and 100-year return periods of peak discharge was computed in the model using Manning's formula by considering gradually varied flow (direct step iteration method). The scenarios for maximum discharge of 2-year, 10-year, 50-year, and 100-year return periods are discussed below.

The water surface profile for 2-, 10-, 50-, and 100-year return periods of peak discharge was computed in the model using Manning's formula by considering gradually varied flow (direct step iteration method). The scenarios for maximum discharge of 2-year, 10-year, 50-year, and 100-year return periods are discussed below.

A. 2-year and 10-year return period design discharge scenarios

From the results shown in the model, the 2-year and 10-year design discharges were nearly accommodated within a floodplain limit in all reaches of the Mersa station except for some reaches that had small riverbanks under one or both banks.

Generally, the problem was more frequently observed in the upper reach because of bank height differences and in the downstream reach because both had small bank heights on both sides compared to the preceding river reach in addition to the bank height differences. However, there are reaches that would accommodate the design discharge of all recurrence intervals within the floodplain limit.

Flood Plain Delineation

A flood inundation map is prepared using both HEC-RAS and HEC-GeoRAS (ArcGIS extension), and the following sequential step is followed to obtain a flood plain map.

A flood inundation map was generated after postprocessing in HEC-GeoRAS with input water surface elevations TIN and cross-section (XS) cut lines within the limits of the bounding polygon. Floodplain mapping was completed after water surface generation and flood plain delineation using a raster.

Sediment Transport Computations

To simulate the sediment analysis or riverbed change in the channel, quasiunsteady flow is used. Its capabilities are unique to sediment transport analysis and simulate the flow series by assuming an approximate continuous hydrograph (histograms) with a sequence of steady flow computations in corresponding flow durations (Brunner 2016). From 17-year recorded flow data, the 7-year daily flow events that start from January 01, 2006 to December 31, 2012 are used for this study to model the simulation of sediment. The annual hydrograph selected is discretized to a series of daily flows. Daily discretized flow records and daily temperature are required in quasiunsteady sediment transport analysis for this study, and 7-year daily flow events out of 17-year recorded flow data, and 7-year average daily temperature of Mersa are used for analysis starting from January 01, 2006 to December 31, 2012. Additionally, hydrograph data of both daily discharge and average daily temperature are presented as follows.

Bank Stability and Toe Erosion Model (BSTEM) Analysis

Riverbank failure clearly led to life and property losses. According to Arora (2008), it is essential to check channel stability through a recent soil testing method and stability analysis. In this study, as discussed earlier, a soil sample was taken from the bank for the triaxial compression test to determine the soil parameters, and BSTEM was used for stability analysis. Bank stability and toe erosion models are bank failure analyses that depend on fundamental force stability, with a toe scour model that allows response between the hydraulic hydrodynamics on the bank toe, which could exacerbate the failure risk during toe scour or decrease failure risk during toe protection (CEIWR-HEC 2015). The aims of HEC-RAS with BSTEM are to construct a model that simulates the responses between riverbanks and bed processes. BESTEM input data are all the data that were used in the sediment analysis, and additionally, the right and left edge and toe station, selection of the corresponding bank failure method and ground water method and BESTEM layer parameters or soil parameter (c and ϕ) are needed. In this thesis, the method of bank failure is the slice method because it is more conventional geotechnical to planer failure and ensures that the force and momentum balance calculated for individual segments of the failure plane is closer to comparable geotechnical analysis and computes a more realistic distribution along the failure plane (CEIWR-HEC 2015). The ground water elevation for BSTEM is taken as 200 m below the ground surface, and these data are obtained from the AWWDS, which is the average ground water elevation in the study area.

Channel Stability Evaluation

Channel stability can be evaluated by assessing the channel bed change, channel bank variation and water surface profile for different recurrence intervals to check its effect over the neighboring area. Thus, the evaluation system is described in detail in the next section.

Channel Bed Stability Analysis

Different methods have been used to simulate sediment transport. This selection was based on the soil composition of the study watershed or catchment. In this study, Meyer Peter Muller and Yang used a sediment transport simulation model with 7 years of daily flow and temperature data. In the HECRAS manual for sand and gravel soil material, the Yang and Meyer Peter Muller transport function is recommended. The simulation results show that aggradation and degradation were observed together along the Mersa River reach. Channel bed change in the Mersa River was checked in two ways: one evaluating the vertical bed change and the other assessing the quantity of sediment entry with sediment leaving.

Vertical Channel Bed Change

The vertical channel bed change simply indicates the amount of erosion or deposition at depth. According to the Yang sediment transport formula, the aggradation and degradation simulated results for the 7-year daily discharge of the Mersa River reach are tabulated and plotted as follows. A maximum deposition of 2.23 m at station 28 and an extreme degradation of 2 m at station 7 were observed. An average degradation of 1.31 m and an average aggradation of 1.09 m were recorded, so the outcomes show that the degradation pattern is somewhat greater than the aggradation in the Mersa River reach.

As presented in Table 9.6, even if aggradation and degradation were observed, some cross-sections also neither aggraded nor degraded at stations 27, 29, 33… can be mentioned by the Yang sediment transport method.

Generally, Yang's transport method result could be grouped under category one: There was no aggradation or degradation from both banks, but deposition or erosion was observed in the channel bed. Second, no aggradation or degradation at the left and right banks, including the channel bed, was observed, and the remaining aggradation or degradation was observed at the right and left banks in addition to the channel bed.

It was found that there was no aggradation and degradation or erosion in the riverbank, whereas degradation was observed at the channel bed only.

Table 9.6 Channel bed elevation change according to Yang

No.	River	Reach	RS	Elevation (m) @Jan 1, 2006	Elevation (m) @Dec 31, 2012	Difference (m)
1	Mersa	All reach	42	1776.981	1775.675	− 1.31
2	Mersa	All reach	41	1775.755	1773.759	− 2.00
3	Mersa	All reach	40	1774.207	1772.916	− 1.29
4	Mersa	All reach	39	1772.954	1772.444	− 0.51
5	Mersa	All reach	38	1771.871	1769.874	− 2.00
6	Mersa	All reach	37	1770.617	1770.581	− 0.04
7	Mersa	All reach	36	1768.513	1766.514	− 2.00
8	Mersa	All reach	35	1767.059	1767.059	0.00
9	Mersa	All reach	34	1765.785	1765.785	0.00
10	Mersa	All reach	33	1764.21	1764.21	0.00
11	Mersa	All reach	32	1762.539	1762.539	0.00
12	Mersa	All reach	31	1761.182	1761.182	0.00
13	Mersa	All reach	30	1759.98	1759.146	− 0.83
14	Mersa	All reach	29	1758.247	1757.622	− 0.62
15	Mersa	All reach	28	1756.402	1758.631	2.23
16	Mersa	All reach	27	1755.367	1755.377	0.01
17	Mersa	All reach	26	1751.532	1752.479	0.95
18	Mersa	All reach	25	1752.921	1750.922	− 2.00
19	Mersa	All reach	24	1751.589	1751.097	− 0.49
20	Mersa	All reach	23	1750.289	1748.29	− 2.00
21	Mersa	All reach	22	1748.751	1747.794	− 0.96
22	Mersa	All reach	21	1747.705	1747.705	0.00
23	Mersa	All reach	20	1745.997	1743.999	− 2.00
24	Mersa	All reach	19	1744.521	1743.486	− 1.04
25	Mersa	All reach	18	1743.531	1743.531	0.00
26	Mersa	All reach	17	1741.037	1741.285	0.25
27	Mersa	All reach	16	1738.831	1738.831	0.00
28	Mersa	All reach	15	1736.616	1735.484	− 1.13
29	Mersa	All reach	14	1736.084	1736.084	0.00
30	Mersa	All reach	13	1733.537	1732.767	− 0.77
31	Mersa	All reach	12	1731.328	1733.126	1.80
32	Mersa	All reach	11	1730.245	1728.246	− 2.00
33	Mersa	All reach	10	1728.954	1728.954	0.00
34	Mersa	All reach	9	1720.103	1722.112	2.01
35	Mersa	All reach	8	1718.622	1719.835	1.21
36	Mersa	All reach	7	1716.877	1714.877	− 2.00

(continued)

Table 9.6 (continued)

No.	River	Reach	RS	Elevation (m) @Jan 1, 2006	Elevation (m) @Dec 31, 2012	Difference (m)
37	Mersa	All reach	6	1714.803	1715.432	0.63
38	Mersa	All reach	5	1712.324	1713.181	0.86
39	Mersa	All reach	4	1709.991	1710.383	0.39
40	Mersa	All reach	3	1707.437	1709.068	1.63
41	Mersa	All reach	2	1705.965	1705.965	0.00
42	Mersa	All reach	1	1703.185	1703.027	− 0.16

Another method that was used in this investigation, Meyer Peter and Muller, gave an acceptable result in aggradation compared to field observations, and for the same fashion as the Yang sediment transport formula, the simulation for 7-year daily discharge in the study reach was performed, and deposition or degradation was observed in various reaches of the Mersa River. Accordingly, Meyer Peter and Muller reported a maximum aggradation or deposition of 3.33 m at station 26 and degradation of 2 m at stations 5, 7, 11, 25, 31, 36, and 41, as shown in Table 9.7. Additionally, the average aggradation was 1.12 m, and the degradation was also 1.52 m, thus showing that the Mersa reach was more disposed of by erosion.

When we compare the simulation results of both transport functions (Yang's and Meyer Peter Muller's methods), nearly half of the river reaches had similar or the same channel bed changes, especially on channel reaches that were neither aggraded nor degraded, and some reaches had the same degradation.

For station 30, deposition was observed near the left riverbank, at channel degradation and on the right riverbank aggradation. Additionally, the trend of aggradation and degradation for the complete 7-year daily discharge simulation, as shown in the figure below, shows that only for the first year to half of a year was the trend not uniform after half of 2006 to the end of 2012. At station 29 near both banks, large aggradation was observed, while in the middle of the reach, small aggradation and degradation were observed.

According to the above two scenarios (Yang transport method and Meyer Peter and Muller transport method), the results could be grouped into three conditions as follows. The initial condition near 49% of the Mersa River reach had equivalent results on both transport methods, the second condition near 46% of the Mersa River reach also had similar results, and the remaining 5% of the Mersa River reach had the opposite mean on one method of deposition on the other degradation. Finally, which works better or is acceptable for the reach of the channel must be determined to help recommend appropriate mitigation measures to change the channel bed. To differentiate the appropriate method for studying rivers, reach field observations and sample cross-sections surveyed one year later in January 2020 (the same benchmark as before) were compared with the one-year model results from both methods. The aggradation or degradation data were surveyed in 2019, and later 2020 is shown in Table 9.8 below for selected river reaches upstream and downstream.

Table 9.7 Channel bed elevation according to MPM

River	Reach	RS	Elevation (m) @Jan 1, 2006	Elevation (m) @Dec 31, 2012	Difference (m)
Mersa	All reach	42	1776.981	1775.391	− 1.59
Mersa	All reach	41	1775.755	1773.756	− 2.00
Mersa	All reach	40	1774.207	1772.908	− 1.30
Mersa	All reach	39	1772.954	1771.409	− 1.54
Mersa	All reach	38	1771.871	1769.882	− 1.99
Mersa	All reach	37	1770.617	1770.894	0.28
Mersa	All reach	36	1768.513	1766.514	− 2.00
Mersa	All reach	35	1767.059	1767.059	0.00
Mersa	All reach	34	1765.785	1765.785	0.00
Mersa	All reach	33	1764.21	1764.21	0.00
Mersa	All reach	32	1762.539	1762.539	0.00
Mersa	All reach	31	1761.182	1759.182	− 2.00
Mersa	All reach	30	1759.98	1759.819	− 0.16
Mersa	All reach	29	1758.247	1758.062	− 0.19
Mersa	All reach	28	1756.402	1757.478	1.08
Mersa	All reach	27	1755.367	1753.367	− 2.00
Mersa	All reach	26	1751.532	1754.864	3.33
Mersa	All reach	25	1752.921	1750.922	− 2.00
Mersa	All reach	24	1751.589	1751.74	0.15
Mersa	All reach	23	1750.289	1748.462	− 1.83
Mersa	All reach	22	1748.751	1747.479	− 1.27
Mersa	All reach	21	1747.705	1747.705	0.00
Mersa	All reach	20	1745.997	1744.553	− 1.44
Mersa	All reach	19	1744.521	1743.691	− 0.83
Mersa	All reach	18	1743.531	1743.531	0.00
Mersa	All reach	17	1741.037	1741.221	0.18
Mersa	All reach	16	1738.831	1738.831	0.00
Mersa	All reach	15	1736.616	1735.5	− 1.12
Mersa	All reach	14	1736.084	1736.084	0.00
Mersa	All reach	13	1733.537	1731.953	− 1.58
Mersa	All reach	12	1731.328	1731.842	0.51
Mersa	All reach	11	1730.245	1728.246	− 2.00
Mersa	all reach	10	1728.954	1728.954	0.00
Mersa	All reach	9	1720.103	1718.157	− 1.95
Mersa	All reach	8	1718.622	1717.941	− 0.68
Mersa	All reach	7	1716.877	1714.877	− 2.00

(continued)

Table 9.7 (continued)

River	Reach	RS	Elevation (m) @Jan 1, 2006	Elevation (m) @Dec 31, 2012	Difference (m)
Mersa	All reach	6	1714.803	1714.83	0.03
Mersa	All reach	5	1712.324	1710.325	− 2.00
Mersa	All reach	4	1709.991	1711.2	1.21
Mersa	All reach	3	1707.437	1710.733	3.30
Mersa	All reach	2	1705.965	1705.965	0.00
Mersa	All reach	1	1703.185	1701.585	− 1.60

Table 9.8 One-year simulation result and field survey collected data comparison

Channel bed change	River reach	Sediment transport formula		Field surveyed cross-section
		1 year simulation result (m/year)		1 year later collected (m/year)
		Yang	Meyer Peter and muller	
Aggradation	Upstream reach	1.12	1.08	1.07
	Downstream reach	0.22	1.21	0.21
Degradation (negative)	Upstream reach	1.18	2	1.16
	Downstream reach	2	1.83	1.94

A comparison between the simulation result and the reality in the field is shown in Table 9.8. The result of upstream reach aggradation or deposition according to Meyer Peter and Muller (MPM) and Yang compared to the field observations Yang overestimated, but MPM best fit, the aggradation of the upstream river reach. Downstream reach aggradation compared to site aggradation was fitted to Yang rather than MPM because it overestimates deposition. Degradation in both the upstream and downstream reaches was fitted with the Yang sediment transport formula rather than the MPM transport function. According to the MPM results, degradation upstream overestimates the realistic situation, while in the downstream reach, it underestimates the field observations. In conclusion, Yang gives a more realistic vertical change than MPM; therefore, the Yang sediment formula was the best representative transport function for our Mersa River reach.

Sediment Quantity Change

As discussed above, there was a vertical change or that the channel was obviously not stable. In addition to these vertical changes, the quantity of sediment entry (mass entry) and sediment leave (mass leave) in the channel must be explained. Therefore,

the mass input to the Mersa River and mass leave in each year from the Mersa River are presented in Table 9.9.

Table 9.9 shows the amount of sediment mass change in the channel, and the negative sign and positive sign indicate erosion and deposition, respectively; the cumulative mass in and out from the channel is shown in Appendix D. Finally, the Mersa River was affected by erosion rather than deposition, with an average cumulative sediment eroded from the channel of 22,470 tons per year. The delineated Mersa catchment was under the subbasin Awash Terminal, and according to ARBA (2017), the total erosion generated from this subbasin or Awash Terminal was 38.2 Mt/yr. The result obtained from the Mersa River was 22.47, which is acceptable.

Channel Bank Stability Analysis

As mentioned in the previous chapter, the bank stability and toe erosion model simulation was performed with a static ground water table for the ground water method, and the bank failure method was performed with the slice method. The BSTEM analysis results show that all Mersa River reach factors of safety were greater than unity except at reaches 33 and 26, where the safety factor was 0 for the right bank and left bank, respectively. Both the right and left banks were stable (no bank failure), and there was also no toe erosion. The stability conditions at both the bank and toe stations were stable against severe erosion. Table 9.10 and Fig. 9.9 show the shear stress produced by flow for the entire simulation period (from 2006 to 2012). The maximum or extreme shear stress was 152 Pa at river reach 23 in 2008, and the average shear stress was 10.6 pa.

Summary

Channels dynamically change in response to variations in flow and sediment transport. This change may cause the destruction of infrastructure, farmland, and property losses. Therefore, channel stability should be assessed, and appropriate stabilization measures should be provided to prevent such damage. This study tried to cover hydrological and hydraulic analyses to investigate the Mersa riverbed and bank stability. An L-moment diagram was used to identify the best fit distribution for gauged data, and out of 12 equations plotted in the diagram, the recorded data were fitted to the general extreme value method (Gumbel's method). Peak floods were estimated using the general extreme value frequency analysis method based on 17 years of stream flow data, and peak discharges for return periods of 2 years, 10 years, 50 years, and 100 years were 41 m^3/s, 68 m^3/s, 91 m^3/s, and 101 m^3/s, respectively.

Sieve analysis and triaxial compression tests were performed to determine the particle size gradation curve and BSTEM parameters, respectively. A gradation curve was used to determine the channel bank and bed material composition and in sediment

Table 9.9 Sediment mass in and out difference (tones)

RS	Station (m)	Year						
		2006	2007	2008	2009	2010	2011	2012
42	0.0	− 165.0	14.9	149.5	181.5	181.5	183.2	184.6
41	67.3	− 110.3	66.7	240.0	285.3	289.5	292.6	305.8
40	106.0	684.9	1018.0	1202.8	1355.2	1369.1	1428.4	1457.7
39	182.0	1104.6	1375.0	1658.9	1683.4	1686.7	1732.9	1756.2
38	249.1	1434.5	2029.9	2332.1	2469.2	2486.4	2501.4	2539.1
37	282.7	1884.8	2231.3	2571.0	2608.5	2609.7	2610.4	2625.4
36	363.0	214.8	15.9	122.9	− 36.9	− 36.9	− 36.9	− 27.9
35	444.7	1158.1	1702.2	2159.6	2211.0	2211.7	2212.0	2233.2
34	518.7	4321.3	4096.5	1956.1	1800.2	1805.9	1808.5	1858.8
33	600.9	− 367.6	62.1	66.9	66.9	66.9	66.9	80.6
32	641.7	677.4	654.3	654.4	654.4	654.4	654.4	528.1
31	714.7	2580.6	3085.7	3091.3	3091.3	3091.3	3091.4	3114.7
30	776.6	1728.1	706.2	− 508.9	− 988.6	− 1183.2	− 1362.8	-647.8
29	866.8	-4733.3	-4451.3	− 4451.3	− 4451.3	− 4451.3	− 4451.3	− 4451.3
28	932.2	− 4676.8	− 4772.8	− 4765.1	− 4746.6	− 4734.1	− 4717.5	− 4707.5
27	1022.6	− 1531.3	− 1357.7	− 1357.7	− 1357.1	− 1357.1	− 1357.1	− 1355.6
26	1100.3	2177.0	− 1494.2	− 1494.2	− 1465.7	− 1459.7	− 1459.6	− 1387.4
25	1164.0	− 713.6	− 711.5	− 711.5	− 711.4	− 711.4	− 711.4	− 711.3
24	1230.8	− 2012.1	− 1966.9	− 1858.0	− 1826.5	− 1764.2	− 1709.9	− 1651.7
23	1298.4	− 2330.2	− 2330.2	− 2330.2	− 2330.2	− 2330.2	− 2330.2	− 2335.4
22	1351.2	281.0	282.0	282.0	282.1	282.2	282.2	286.9
21	1394.2	− 672.3	− 631.4	− 620.4	− 605.0	− 598.7	− 598.3	− 589.6
20	1437.9	− 463.5	− 463.5	− 463.5	− 463.5	− 463.5	− 463.5	− 463.5
19	1513.5	− 493.4	− 163.8	56.0	276.1	374.5	446.0	812.4
18	1595.6	− 1477.7	− 1480.0	− 1407.3	− 1480.9	− 1458.0	− 1439.8	− 1573.7
17	1673.3	2726.1	2758.3	2637.7	2841.9	2851.9	2987.2	1372.0
16	1718.3	2422.8	4368.5	8311.5	9405.9	9567.4	9442.3	9377.0
15	1767.7	8494.5	10,442.2	7791.3	7373.7	7336.0	7375.9	7381.5
14	1814.2	4675.7	5525.4	4422.8	3489.8	2881.4	2352.3	2350.8
13	1865.5	91.0	− 3272.1	− 4531.5	− 5957.0	− 6674.4	− 7682.1	− 8623.3
12	1948.0	− 5018.1	− 7389.9	− 7389.9	− 7389.9	− 7389.9	− 7389.9	− 7389.9
11	2004.8	− 6025.0	− 6025.0	− 6025.0	− 6025.0	− 6025.0	− 6025.0	− 6025.0
10	2088.2	− 9560.6	− 9560.6	− 9560.6	− 9560.6	− 9560.6	− 9560.6	− 9560.6
9	2140.5	− 4652.4	− 4652.4	− 4652.4	− 4652.4	− 4652.4	− 4652.4	− 4652.4
8	2197.4	− 939.7	− 938.5	− 937.0	− 937.0	− 937.0	− 937.0	− 937.0
7	2240.0	− 760.4	− 757.0	− 757.0	− 757.0	− 757.0	− 757.0	− 757.0

(continued)

Table 9.9 (continued)

RS	Station (m)	Year						
		2006	2007	2008	2009	2010	2011	2012
6	2297.6	− 762.0	− 757.4	− 757.2	− 757.2	− 757.2	− 757.2	− 757.2
5	2338.3	− 830.8	− 864.4	− 864.4	− 864.4	− 864.4	− 864.4	− 864.4
4	2419.5	− 317.8	− 272.7	− 260.6	− 260.6	− 260.6	− 260.6	− 260.6
3	2485.5	− 1467.3	− 2453.4	− 2768.6	− 2768.6	− 2768.6	− 2768.6	− 2768.6
2	2555.9	− 1875.7	− 1875.7	− 1875.7	− 1875.7	− 1875.7	− 1875.7	− 1875.7
1	2618.4	− 973.7	− 973.7	− 973.7	− 973.7	− 973.7	− 973.7	− 973.7

transport analysis to assess the channel bed change. Triaxial compression tests were performed at 50 kN, 100 kN, and 200 kN loads in the laboratory, and the BSTEM parameters cohesion, C = 5.46 kPa, and angle of shearing resistance, $\phi = 140$, were determined from Mohr's circle after the results obtained from the triaxial compression test were drawn.

The HEC-RAS model was developed with the above inputs, such as the design flood for steady flow analysis for water surface profile computation using the direct step standard method. The result shows that there is overtopping on the bank edge, and adjacent areas were affected due to floods.

Sediment transport simulation and BSTEM analysis were simulated to assess channel bed stability and investigate channel bank conditions. The Mersa River reach exhibits both aggradation and degradation. In the upper reach, the maximum aggradation is 1.08 m at reach 28 over the entire simulation period, while the lower reach reaches 2.01 m at reach 9. The maximum degradation, both at the upper reach and lower reach, is 2 m at different reaches for the entire simulation period. The amount of sediment erosion generated from the study channel is on average cumulative at 22.47 kt/yr. However, both aggradation and degradation observed in the Mersa River channel bed are affected by erosion or degradation more dominantly than aggradation, and the total Mersa River channel bed is unstable.

The BSTEM model analysis results show that there was no erosion on the bank toe, and the safety factor was greater than one except at reaches 33 and 26. It can be concluded that the channel bank of the Mersa River reach is stable. Generally, from the Mersa River investigation, the channel bed is unstable, the bank is stable, and the area adjacent to the river is adversely affected by floods, as analyzed in the water surface profile. To minimize flood impact and stabilize the channel bed, appropriate stabilization measures are recommended. Vertical gabion bank for controlling flood in prone area, check dam and drop structure for stabilizing channel bed based on reach degradation.

Table 9.10 Mersa River reach shear stress

River	RS	Shear Stress (pa)						
		2006	2007	2008	2009	2010	2011	2012
Mersa	42	6.00	0.80	5.13	0.48	0.48	0.09	0.43
Mersa	41	0.95	6.31	18.07	3.39	3.39	0.80	3.76
Mersa	40	0.84	0.26	1.09	0.14	0.14	0.03	0.13
Mersa	39	8.81	5.48	12.99	4.40	4.40	4.70	4.34
Mersa	38	0.06	0.01	0.80	0.00	0.00	0.00	0.00
Mersa	37	1.43	0.70	4.15	0.45	0.45	0.08	0.41
Mersa	36	0.06	0.01	0.64	0.00	0.00	0.00	0.00
Mersa	35	2.57	0.99	14.14	0.65	0.65	0.33	0.63
Mersa	34	1.77	1.04	2.61	0.52	0.52	0.07	0.47
Mersa	33	1.09	0.63	4.60	0.34	0.34	0.13	0.34
Mersa	32	1.15	0.54	1.02	0.37	0.37	0.03	0.31
Mersa	31	0.37	0.30	4.28	0.16	0.17	0.08	0.17
Mersa	30	2.30	1.04	0.86	1.59	1.59	0.11	1.56
Mersa	29	2.16	0.56	1.86	0.14	0.01	0.00	0.00
Mersa	28	30.69	16.66	45.06	12.59	12.61	10.25	11.97
Mersa	27	2.03	0.43	2.87	0.15	0.15	0.10	0.15
Mersa	26	8.00	4.48	16.66	2.76	2.69	0.64	2.22
Mersa	25	1.31	0.33	1.96	0.06	0.04	0.01	0.01
Mersa	24	1.55	0.94	3.46	0.67	0.68	0.18	0.69
Mersa	23	87.37	49.74	152.27	31.34	31.34	5.99	29.94
Mersa	22	0.24	0.12	1.14	0.09	0.10	0.05	0.12
Mersa	21	4.05	1.72	9.37	0.94	0.94	0.17	0.89
Mersa	20	2.62	1.25	2.39	0.77	0.77	0.19	0.74
Mersa	19	0.11	0.04	0.64	0.02	0.02	0.00	0.03
Mersa	18	5.37	3.23	9.65	2.00	2.00	0.53	1.92
Mersa	17	1.95	0.98	5.24	0.61	0.61	0.12	0.59
Mersa	16	4.55	2.19	7.72	1.37	1.37	0.42	1.30
Mersa	15	0.07	0.03	1.15	0.01	0.01	0.00	0.01
Mersa	14	3.50	3.09	5.20	2.26	2.26	0.81	2.59
Mersa	13	0.53	0.13	0.23	0.00	0.00	0.00	0.00
Mersa	12	3.25	3.11	5.99	2.26	2.26	0.41	2.58
Mersa	11	0.32	0.05	2.87	0.01	0.01	0.00	0.01
Mersa	10	4.07	2.50	8.72	1.60	1.60	0.54	1.33
Mersa	9	1.46	0.74	4.16	0.49	0.49	0.11	0.44
Mersa	8	8.58	4.71	11.92	2.79	2.79	1.31	3.10
Mersa	7	2.90	0.87	4.53	0.36	0.40	0.03	0.34

(continued)

Table 9.10 (continued)

River	RS	Shear Stress (pa)						
		2006	2007	2008	2009	2010	2011	2012
Mersa	6	3.81	2.03	13.27	3.66	1.32	0.40	3.97
Mersa	5	7.79	3.80	11.77	0.90	2.35	0.47	0.84
Mersa	4	0.66	0.25	1.83	0.64	0.13	0.03	0.61
Mersa	3	5.88	2.99	14.72	2.03	2.04	0.81	1.99
Mersa	2	8.45	4.76	16.33	3.46	3.46	2.16	3.41
Mersa	1	4.45	3.06	7.95	1.86	1.86	0.48	1.80

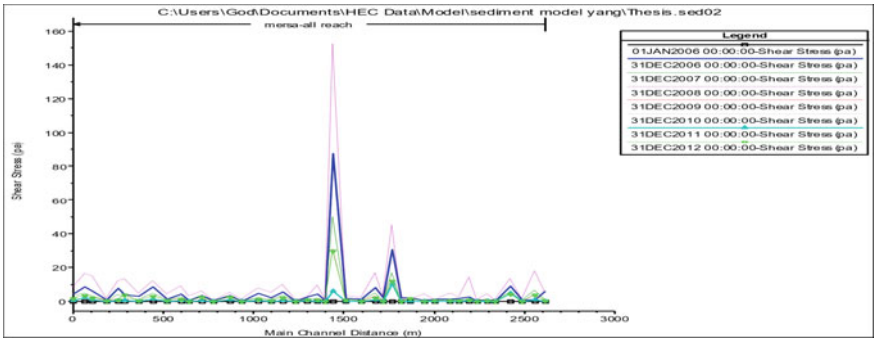

Fig. 9.9 Mersa River shear stress for the simulation period from 2006 to 2012

References

Arora KR (2008) Soil mechanics and foundation engineering (geotechnical engineering): In SI units. Standard publishers

Awash River Basin Authority (2017) Executive summary of strategic river basin plan for Awash Basin

Brunner GW (2016) HEC-RAS river analysis system: hydraulic reference manual, version 5.0. US Army Corps of Engineers–Hydrologic Engineering Center, 547

CEIWR-HEC (2015) HEC-RAS USDA-ARS bank stability & toe erosion model (BSTEM), Technical Reference & User's Manual

Chow VT, Maidment DR, Mays LW (1988) Applied hydrology. McGrawHill, New York

Chow VT (1959) Open channel hydraulics. Caldwell. The Blackburn Press, New Jersey

French RH (1986) Open channel hydraulics. McGraw-Hill New York

Garde RJ, Ranga Raju KG (1978) Mechanics of sediment transportation and alluvial stream problems. Wiley Eastern Ltd, New Delhi

Hawi A (2018) Investigating the effect of scouring on hydraulic performance of cross drainage structure (case study of Ginchi Awash Bridge). Thesis, Addis Ababa University

Hosking JRM (1990) L-moments: analysis and estimation of distributions using linear combinations of order statistics. J Royal Stat Soc

Hosking JRM (1991) Approximations for use in constructing L-moments ratio diagrams, vol 3. Res Report, RC-16635. IBM Res Division, New York

Meyer-Peter E, Müller R (1948) Formulas for bed-load transport. Proc., 2nd Meeting. IAHR, Stockholm, Sweden
Murthy VNS (2002) Geotechnical engineering: principles and practices of soil mechanics and foundation engineering. CRC Press, Boca Raton
Subramanya K (2008) Engineering hydrology. McGraw-Hill, New York